THE PENNSYLVANIA STATE UNIVERSITY
SCHREYER HONORS COLLEGE

DEPARTMENT OF ENGINEERING SCIENCE AND MECHANICS

LOW FIELD ELECTRICALLY DETECTED MAGNETIC RESONANCE

JOSEPH P. ACQUAVIVA
Spring 2011

A thesis
submitted in partial fulfillment
of the requirements
for a baccalaureate degree
in Engineernig Science
with honors in Engineering Science

Reviewed and approved* by the following:

Dr. Patrick Lenahan
Distinguished Professor
Thesis Supervisor

Dr. Tony Huang
Associate Professor
Honors Adviser

Dr. Judith A. Todd
Department Head
Engineering Science and Mechanics

* Signatures are on file in the Schreyer Honors College and the College of Engineering Science and Mechanics

ABSTRACT

Very little literature exists regarding electrically detected magnetic resonance (EDMR) at low fields. EDMR at low fields holds exciting possibilities for device characterization as there is relatively little loss of signal strength at low fields, where there is a very large loss in sensitivity in conventional magnetic resonance at low fields. Furthermore, at least in principle, for signals primarily broadened by spin-orbit coupling, there might actually be significant signal to noise advantages in low field measurements. We tested SiC MOSFETs under magnetic fields ranging from 0 to 50 gauss while exposing them to RF power. The goal is observe spin dependent change in the current through the device which is consistent with the Planck-Einstein equation. After discussing the background theory, we gave a detailed description of the low field EDMR rig used for these experiments, highlighted the component subsystems and stated ways to check each one. Despite the sound theoretical basis for low field EDMR, and apparent proper operation of the individual subsystems, we were unable to obtain an EDMR signal using the low field rig. We highlight an example test which first seemed promising, but failed under scrutiny and explain why. We make note of several of the problems we encountered during the course of experimenting, as well as the steps we took to fix them. We attempt to explain several possible reasons for the inability to obtain an EDMR signal and finally we end with a complete list of steps that must be taken, for in the future, when we do observe EDMR with the current setup.

TABLE OF CONTENTS

ACKNOWLEDGEMENTS iii

Chapter 1 Introduction 1

Background Theory 1
Helmholtz Coils 4

Chapter 2 Experimental Setup 6

RF Power 9
Q value 10
Device Biasing and Current Amplification 12
Modulation 14
Magnetic Field Ramp Generation 18

Chapter 3 Results 20

Problems encountered 20
Initial promising signs 23
Possible Reasons for Failure 24
Future Work 25

Chapter 4 Conclusion 26

Bibliography 27

ACKNOWLEDGEMENTS

Dr. Patrick Lenahan

Brad Bittel

Corey Cochrane

Michael Dunn

Chapter 1

Introduction

Background Theory

Electrically detected magnetic resonance (EDMR) is a type of electron spin resonance (ESR). EDMR is commonly used to determine device limiting defects in semiconductors. EDMR techniques have an advantage over ESR in that they have sensitivity over 10 million times greater [1]. This allows for detection of atomic-scale defects in fully processed transistors [2].

EDMR was first discovered in 1966 by two groups independently, Maxwell and Honig, and Shmidt and Solomon [3]. EDMR measurements have been conducted on many types of semiconductor devices, to great success in determining the underlying defects present within them, which limit performance. Among these are Si diodes under a variety of conditions (plastically deformed, amorphous Si, Hydrogenated, and iron-contaminated), Si p-i-n solar cells, light emitting diodes, III-V semiconductor devices, Silicon Carbide, and even organic field effect transistors [4] [5].

EDMR is by nature more sensitive than conventional ESR because it measures a change in voltage or current, whereas ESR measures absorption or dispersion within the microwave cavity. Kaplan, Solomon, and Mott [1] proposed a model to account for the much larger signal strength of EDMR over ESR based on a difference in the mechanism of recombination [2]. The KSM model assumes Shockley-Read-Hall recombination processes, in which electrons and holes are first captured at a recombination center. There, they form pairs, and remain that way for a relatively long period of time before recombining. Recombination can only occur of the pairs are

of opposite spin, called “singlet pairs.” Otherwise, they must disassociate into free electrons and holes, designated “triplet pairs.” These stable triplet pairs occupy the recombination centers, further blocking recombination. At resonance, these triplet pairs are converted into singlet pairs, greatly enhancing the recombination rate [3].

To observe small Spin-dependent recombination (SDR), non-equilibrium carrier concentration must first be present. Typically, this is accomplished by applying a forward bias to a transistor junction or diode. EDMR is extremely useful in the characterization of the defects present not only bulk materials but already-manufactured semiconductor devices [3].

There has been very little study using EDMR at low fields even though, as will be shown below, the theoretical signal strength is essentially independent of the magnitude of the magnetic field. This means that the potential benefits of using EDMR at low field are two fold. The first potential saving is in cost. It is relatively straightforward and inexpensive to build from scratch a set of Helmholtz coils capable of producing a magnetic field on the order of 50-60 Gauss. Compare this to a conventional electromagnet and the necessary microwave cavity, which cost on the order of $100,000. The assorted other lab apparatus required, such as a Gaussmeter, a lock-in amplifier, a signal averager, several signal generators, and amplifiers can be obtained for under $10,000, and all of these pieces of equipment are necessary anyway for standard EDMR. This is an effective order of magnitude drop in the cost of a device to perform EDMR, significantly lowering the barrier for semiconductor research.

The second benefit is that for wide signals, in which the line width is primarily due to spin-orbit coupling, using using a low field for EDMR actually increases the theoretical signal strength, making it actually preferable to conventional EDMR in certain applications.

Silicon Carbide metal oxide field effect transistors (SiC MOSFETs) in particular hold great promise for high power and high temperature applications because of the wide bandgap of SiC [6]-[9]. Until recently, the limiting defects of SiC devices were not well understood, but

recently, it has been determined that the nature of SiC defects is more complex than the ones present in conventional silicon devices [10], [11].

To conduct EDMR measurements, an appropriately biased device is placed in the presence of a slowly varying magnetic field and a radio-frequency (RF) magnetic field. According to the equation, $\Delta E=h\nu=g\beta H$, where h is Planck's constant, ν is the radio frequency, g is a second rank tensor, β is the Bohr Magneton, and H is the magnetic field at resonance, an EDMR signal will be present at the magnetic field corresponding to the RF frequency as well as the g value.

The value of g depends on the relationship between the magnetic field vector and the defect being observed, it is properly expressed as a matrix, sometimes called the 'g tensor' [12].

By applying a slowly varying (constant) magnetic field, unpaired electrons' spins will be aligned to either parallel or anti-parallel MS = +1/2 or -1/2 respectively, to the applied field. Based on a principle called the Zeeman effect, the energy of the spin system is split into two levels at this point. This is illustrated in Figure 1. Because of the Pauli exclusion principle, no two electrons in a single system can share the same quantum numbers. Due to this fact, EDMR signals are present primarily when the defect involves an odd number of electrons (paramagnetic defects), such as a dangling bond, however certain ESR active defects with an even number of electrons may also be observed [2].

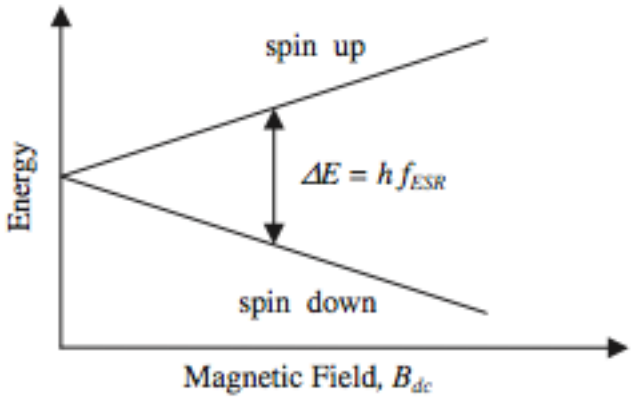

Figure 1: The difference in energy between spin up and spin down as a function of magnetic field [3].

As will be shown later, however, the larger difference in energy does not, in and of itself, cause an increase in SDR signal strength. Surprisingly little literature exists on the study of EDMR at such low fields. This is surprising, given its potential benefits, but also exciting for the possibility of real benefits to applications involving device characterization.

Helmholtz Coils

Hemholtz coils provide a very uniform magnetic field in the region centered between the coils.

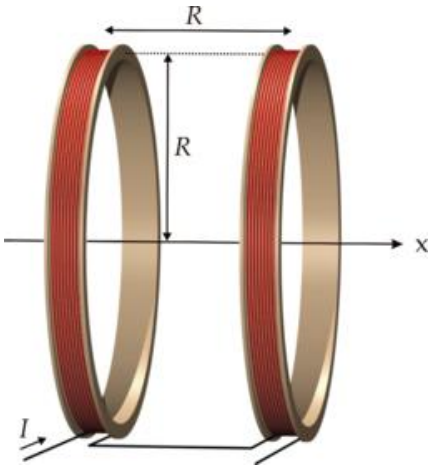

Figure 2. Hemholtz coils schematic

The magnetic field is given by the relationship:

$$B = \frac{.899\, nI}{R}, \tag{1}$$

where R is the radius, n is the number of turns around each coil, I is the current flowing through the coils (in Amperes), and B is the magnetic field in Gauss midway between the coils. This is where the sample to be characterized is placed.

Helmholtz coils are desirable for EDMR measurements because they provide a very uniform magnetic field around the halfway point between the coils. Because of this, and the small physical size of typical devices of transistors, the magnetic field which over which the sample is exposed can be assumed to be uniform.

EDMR typically employs two sets of Helmholtz coils. The larger, outer coils provide the repeated sweeping magnetic field. A smaller set provides what is called the modulation. The largest signals are observed when the modulation amplitude is equal to the peak-to-peak width of the signal.

Chapter 2

Experimental Setup

The Low-Field EDMR rig consists of four interdependent, interlocking systems: The tuned RF circuit, the device biasing and amplifier, the modulation, and the magnetic field sweep. The following table lists the devices used.

Device	Option	Optimum Setting	Cables From	Cables To
Bias Box	Vbias plus or minus	Depends on device under test	Device itself Screw on Right Side Sub/Collector	Upper Left Box Connection Ground Preamplifier Input
Stanford Current Preamplifier	Sensitivity	2 x 1 uA/V	Output	Lock-In Signal Input A
	Gain Mode	Low Noise		
	Filter Freq	10 Hz		
	Filter Type	Highpass 6dB		
	Bias Voltage	Pos		
	Input Offset	Pos 1 x 1 pA		
	Invert	On		
Boonton Signal Generator	Output Level	Max on 1V scale	Output	Top of Tuning Box
	Output Frequency	58 MHz (depends of tuning LC circuit)		
	Modulation FM	Off		
	Modulation AM	Off		
Stanford Lock-In Amplifier	Signal Filters	Bandpass IN Line IN Line x2 IN	Channel 1 Output	National Instruments AI 0
	Signal Inputs	A		
	Sensitivity	500uA		
	Dyn Res	Low		
	Expand	X10		
	Display	X Y		

	Reference	(variable)		
		(variable)		
	Mode	f		
	Trig	Sin Wave		
	Time Constant	Pre: 1 s Post: 1 s		
Kepco Bipolar Power Supply	Current	0 to 2 A	Common Output	Brass Coil APP
Sony Audio/Video Control Center	Speaker	A	Speakers L +/-	Through Resitor Box to Brass Coil MOD
	Output	CD		
	Volume	33-36		

BK Precision Function Generator	Triggered Output	Run	Output LO (split w/ T)	Lock-In Reference Input
	Range	(variable)	Output LO (split w/ T)	Sony CD In
	Frequency	(variable)		
	Wave Shape	Sine Wave		
	DC Offset	Off		
	Amplitude	Max		
	Output	LO		
Laptop / Data Collection Software	Program Ver.	Low Field2.vi		
	Center			
	Scan Width			
	Scan Time	120 s		
	Scan Number	30		
	Gain	18		
National Instruments BNC-2110			Large Top Plug	Laptop
			AO 0	Kepco Voltage Programming Input
LC tuning circuit	Matching Capacitor	Adjust for Max Field	Back Plug	Vertical Coil around Device
	Tuning Capacitor	Adjust for Max Field		

Also included in the overall setup are the device itself being tested, the lock-in amplifier, and the signal averager. The schematic diagram for the system is shown below.

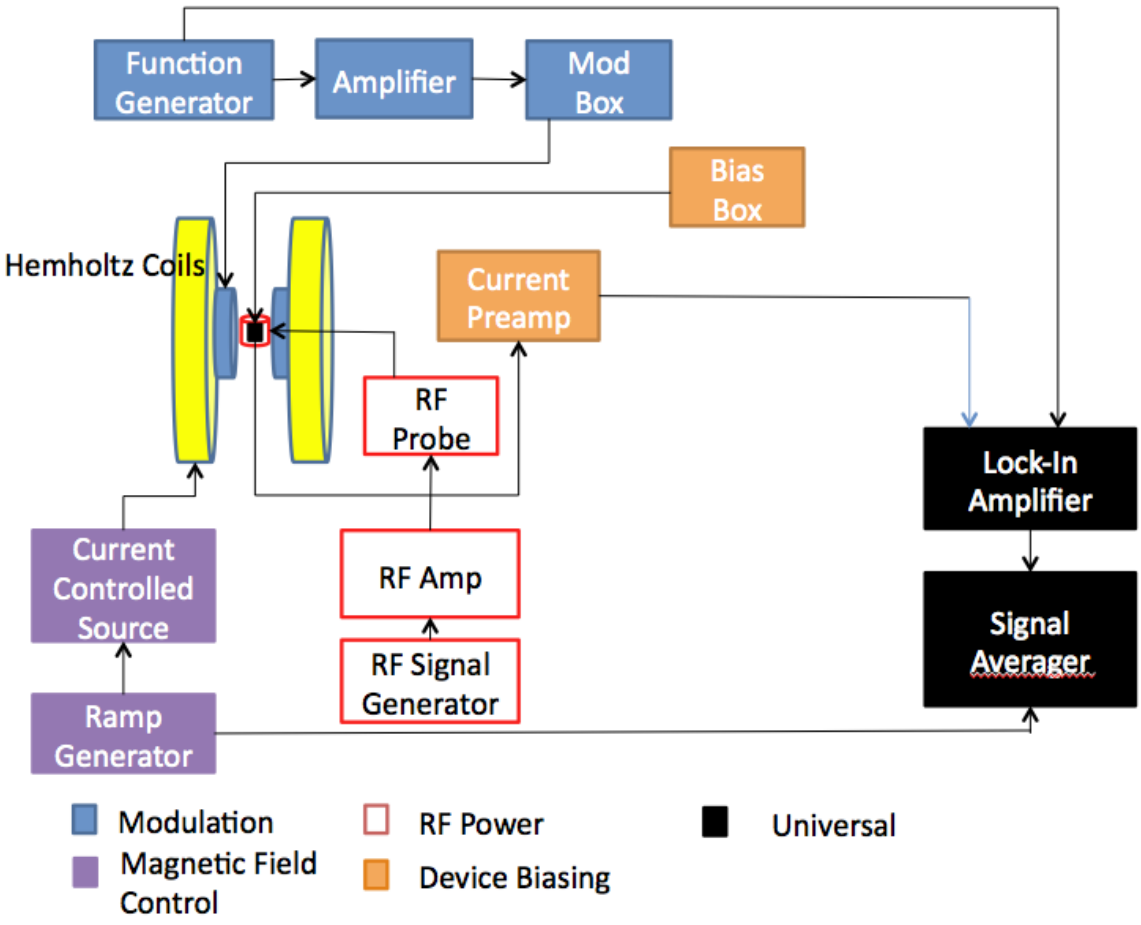

Figure 3: Low Field EDMR rig schematic diagram.

The above diagram illustrates the devices which comprise the system. All subsystems must be operating to observe a signal from the signal averager.

We will now discuss the individual systems in detail, as well as the tests to determine that they are functioning.

RF Power

The RF subsystem consists of the Boonton Signal Generator, the EIN power amplifier, and the LC tuning probe. The LC probe consists simply of two variable capacitors as well as the coil of wire which surrounds the device. Unlike several of the other subsystems, the RF power applied to the device does not have a theoretical optimal value, at which point, increasing the power further will provide no benefit or even decrease the resultant EDMR signal. Therefore, we aim to transmit as much RF power as is feasible with the lab equipment we are using. It is important for the understanding of this subsystem to note that transmitting an AC signal in the Megahertz range over standard coaxial cables is nearly impossible without having to worry about impedance matching. Without impedance matching, there is significant loss of power to the RF coil. To prevent loss, the load at the other end (the RF probe around the device), must have the same characteristic impedance as the signal generator [13].

Also note that the physical system surrounding the RF probe affects the impedance. This necessitates tuning the probe, hence the variable capacitors used. The following is a schematic of the RF probe.

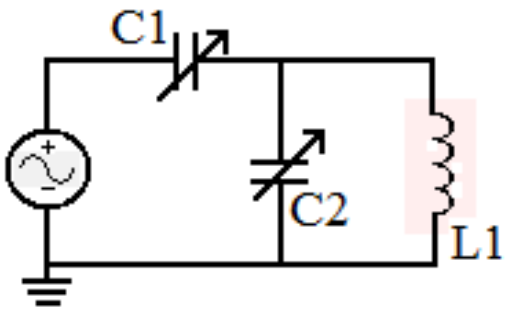

Figure 4: RF Probe

In the diagram, the AC source is the Boonton Signal Generator/Power Amplifier. L1 is an inductor coil surrounding the device being measured, C1 and C2 are variable capacitors. The

device under study, and to a smaller extent, the physical placement of the equipment being used results in an effective change to these capacitance values. In theory, these capacitors should be adjusted to provide minimal signal loss. In practice, adjusting these capacitors by hand did not provide enough precision to accurately tune the probe for an arbitrary frequency. Therefore, we simply adjusted the actual frequency of the RF power being used instead.

By its nature, a simple inductor coil produces the greatest magnetic field directly centered within its coils. Below is an illustration of the magnetic field lines in relation to the RF probe coil (corresponding to L1 above).

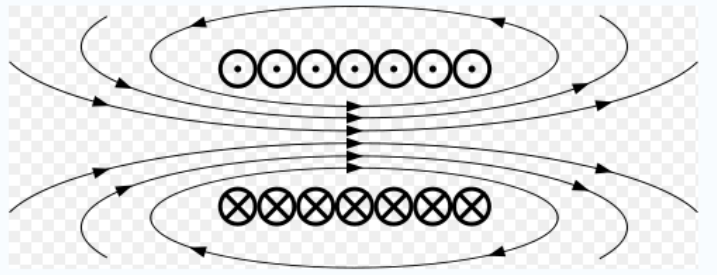

Figure 5: Magnetic Field shape for an inductor coil.

Where the lines are closest together is where the magnetic field is the strongest. It is easy to see, then, that the device under study should be as close to the center of this coil as possible, because of the large dropoff in power when the device is not in the middle of the coil.

The RF Probe which was used included the following: L1 was a 16 gage wire with 7 turns. C1 and C2 were variable capacitors with values 8-80 pF and 10-180 pF, respectively. To maximize the RF power, the quantity we had to measure is called the Q value.

Q value

The Q value is a dimensionless quantity which measures how well the circuit is tuned. The Q value is obtained by measuring the peak amplitude of the RF power, divided by the

frequency corresponding to $1/\sqrt{2}$ of that amplitude. Shown below is a qualitative schematic of the frequency versus amplitude of RF power delivered for a given characteristic impedance.

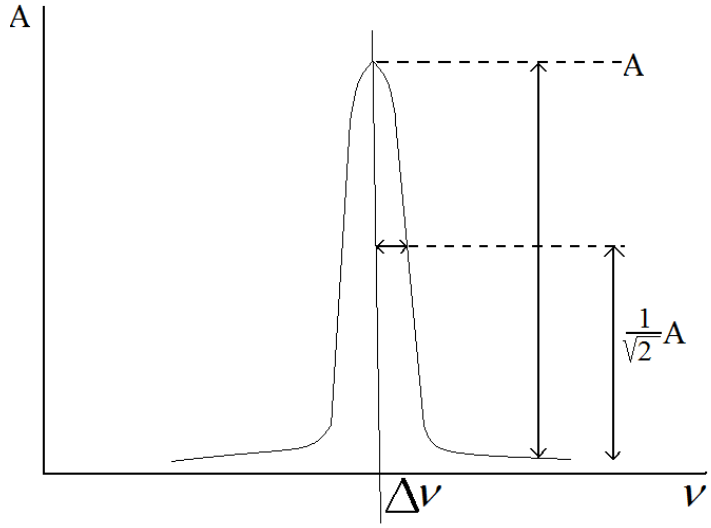

Figure 6: RF frequency vs. Amplitude for a given impedance.

The Q value is given by:

$$Q = \frac{\nu}{2\Delta\nu}, \tag{2}$$

where ν is the frequency which corresponds to the peak amplitude, and $\Delta\nu$ is the difference between the frequency of the peak amplitude and the frequency where the amplitude is $1/\sqrt{2}$ of the maximum.

Measuring these quantities is relatively straightforward. A simple, single turn, inductor coil is placed around the test tube containing the device. It is positioned near, but not right next to the RF probe so that this coil itself is only minimally coupled to the system. This coil is attached directly into an oscilloscope. Upon power-up the oscilloscope will read an AC sinusoid of the same frequency as the signal generator outputs. The peak-to-peak amplitude scales with the amplitude of the magnetic field being delivered to the sample.

Adjusting the variable capacitors, the RF frequency used, and to a lesser extent, the physical positioning of wires and devices of the overall setup, changes the amplitude of the resultant RF magnetic field delivered to the sample. When the device and system is all set up, the RF frequency is adjusted to provide the maximum amplitude. By simply reading the amplitude from the oscilloscope and multiplying by $1/\sqrt{2}$, one may find $\Delta\nu$, and by extension, Q. If the resultant Q value is too low, the variable capacitors are tweaked, in the hopes of better tuning the circuit. Note that if this is done, the optimal RF frequency will invariably change, necessitating adjusting the frequency again to find this new maximum.

When this is done, the circuit is tuned, providing maximum RF power to the device. To achieve decent SNR on an EDMR measurement, the Q value must be on the order of 20. This tuned RF frequency is what we then use to determine the magnetic field at which we should find a signal, by substituting into the relationship hν=gβH.

Device Biasing and Current Amplification

Optimal device biasing is crucial to obtaining a satisfactory EDMR signal. A silicon carbide MOSFET with no gate bias is typically wired such that the source and drain are both at the same forward bias with respect to the substrate (body). Under such a configuration, the device is essentially wired as a p-n junction. Using such a configuration, the resultant recombination current corresponds to the EDMR signal obtained.

Assuming the diode has a uniform distribution of trapping centers, the recombination current, J_r, is, to the first order, given by:

$$J_r = \frac{qn_iW}{2} v_{th} n_t \sigma \exp\left(\frac{qV_a}{2k_bT}\right), \quad (3)$$

Here, $v_{th}$is the thermal velocity, $n_t$is the density of recombination defects, σ is the capture cross section of the defect, and $n_i$is the intrinsic carrier concentration. T is the operating temperature, $k_b$is Boltzman's Constant, and q is the charge of an electron. $V_a$is the applied bias to the diode, and W is the width of the depletion region [2].

W is given by the following equation:

$$W = \left[\frac{2\varepsilon(N_a+N_d)(V_{bi}-V_a)}{qN_dN_a}\right]^{1/2}, \quad (4)$$

Here, ε is the permittivity of the semiconductor, N_a and N_d are the densities of ionized impurity acceptor atoms and ionized donor atoms, respectively. V_{bi} built-in voltage, given by:

$$V_{bi} = \frac{k_bT}{q}\ln\left(\frac{N_aN_d}{{n_i}^2}\right), \quad (5)$$

V_{bi} is constant for a given device (assuming a constant temperature). Likewise, W depends only on V_{bi} and V_a, as all other terms are either material or fundamental constants. In the same way, the expression for J_r can be simplified into a much simpler form.

$$J_r = C * (V_{bi} - V_a)^{1/2}\exp\left[\frac{qV_a}{2k_bT}\right], \quad (6)$$

In this equation, C is the condensed constant values.

It is easy to see, qualitatively, that the recombination current becomes zero at biases greater than the built in voltage. At these large biases, the value obtained for J_r becomes imaginary, losing physical meaning. This is consistent with a physical understanding of the system because at a forward bias greater than the built in voltage of the diode will cause the depletion region, W to become zero, leaving no place for recombination to occur. The SDR signal is proportional to the recombination current by a factor of the spin dependent change in σ (from the original equation), caused by SDR [14]. To obtain the maximum signal, the diode should be biased just under the built-in voltage to obtain the largest recombination current, and therefore,

largest SDR signal. It was determined experimentally by Cochrane, et al. that the for a SiC device with somewhat similar doping densities, -2.35V provides the best SDR response.

These equations also show that, to the first order, the recombination current, and therefore the SDR signal, is independent of the magnitude of magnetic field being used. Because of this, we have a very good theoretical basis for the belief that EDMR using a magnetic field of order 0-60 Gauss is feasible with standard equipment.

The actual bias is provided by a home-built box powered by 9V batteries, across variable resistors. The biased diode is connected in series to a current preamplifier. This is because, even given the exponential relationship between applied voltage and output current of a diode, the resultant current from the diode is typically on the order of μA, when biased for optimal SDR signal. Even though it is in series, the current preamplifier does not need to be taken into account when measuring the diode biasing, because the input is connected to a virtual ground, resulting in a negligible voltage drop. The final output of the current amplifier is given as the input to the lock-in amplifier.

Assuming the device is biased correctly, this subsystem is fairly straightforward to test. When tested by itself, a multimeter can be used to read the output of the current preamplifier. By varying the bias from zero to a few volts, one can plot the I-V curve for the diode. By observing an exponential relationship, we can be relatively certain that the diode is functioning correctly, is wired correctly, is biased correctly, and the current preamplifier is functioning correctly. We can see from this that the diode bias sub system is operating as we would expect, and as we want it to.

Modulation

The purpose of modulation is to turn the DC signal provided from the device into an AC signal of a frequency of our choosing (typically 1 kHz). This AC signal is inputted into the lock-

in amplifier, and with the modulation frequency as a reference, returned to a DC signal. While at first, this may seem completely unnecessary, without using modulation, the signal-to-noise ratio (SNR) is not great enough to observe, even with a very high recombination current. Because the lock-in amplifier only detects signals at the frequency of its reference, a signal at that frequency may be effectively extracted from the background noise. The lock-in is also a phase sensitive detector; it is sensitive only to signals in phase with the reference. This provides an additional boost in sensitivity.

One may be concerned that this AC modulation field may adversely effect the RF power. However, with the device under study, an RF frequency of about 58 MHz, and corresponding magnetic field resonance response at around 21 gauss, a 1 kHz modulation is more than 4 orders of magnitude lower in frequency than the RF power. For the purposes of the physics underlying the SDR signal, it is effectively DC, so this worry is unfounded.

The modulation is provided by a smaller set of Helmholtz coils within the large pair. A waveform generator drives a sinusoidal wave at 1 kHz frequency. The signal is then amplified by a commercial sound system amplifier, and then connected in series with a 10 Ω resistor, a 2 A 250 V fuse, and the modulation coils. The schematic for the circuit is provided below:

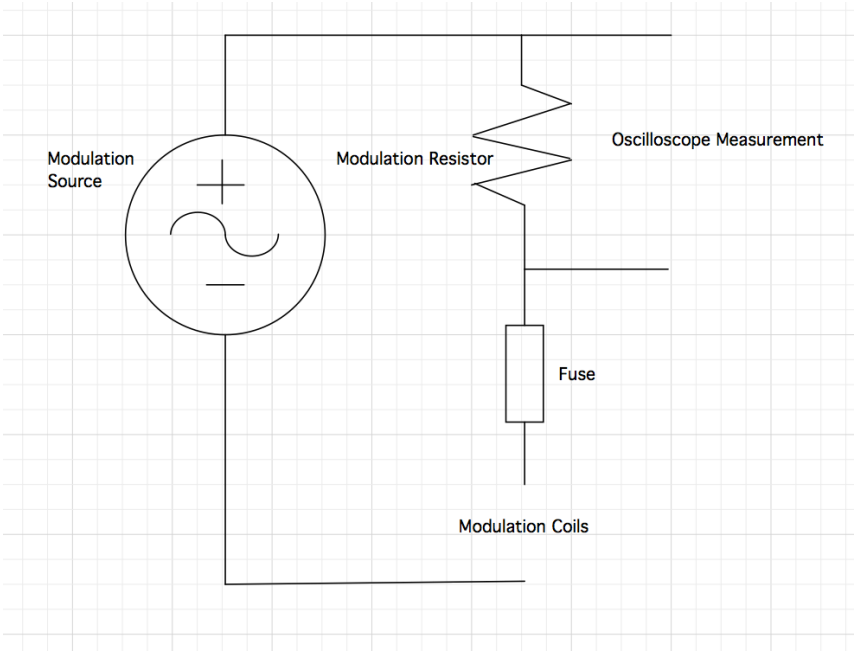

Figure 7: Modulation Circuit Diagram

The purpose of the amplifier is twofold. First, a standard function generator is not capable of producing a large enough peak-to-peak current to achieve the modulation needed. Second, the function generator has an internal resistance of 500 Ω. The modulation coils are simple wire, with an overall resistance of less than 1 Ω.Simply connecting it in to the Hemholtz coils, (and 10 Ω worth of resistance) would result in all the voltage drop occurring across the internal resistance of the function generator, giving effectively zero modulation to the device itself.

A commercial amplifier is built for the output to be attached to sound speakers, which have a resistance from 1-10 Ω. In the case of the Sony, this is 8 Ω. Thus, the internal resistance of the amplifier is much less, and better tuned to drive a low resistance load, and a 10 Ω resistor almost perfectly matching this value.

Like the larger set of Hemholtz coils, the magnetic field provided by the modulation coils is determined by the current, rather than the voltage. Since it is easier to measure voltage than current, an oscilloscope measures the voltage drop across the resistor. With Ohm's Law, we determine the AC current flowing through the modulation coils by dividing the pea-to-peak

voltage by the resistance of the resistor (10 Ω). For example, a 1 V pk-pk AC signal across the resistor corresponds to 100 mA pk-pk.

Because we know the magnitude of the magnetic field we wish to obtain from the modulation coils, we first run a DC current through the coils and measure the resulting field using a Gauss meter. A DC current directly corresponds to an AC current, peak-to-peak, so we can determine the DC current necessary to obtain that magnitude of a magnetic field. That is exactly the same as the AC current, peak-to-peak, which in turn, directly corresponds to the pk-pk voltage drop across the resistor.

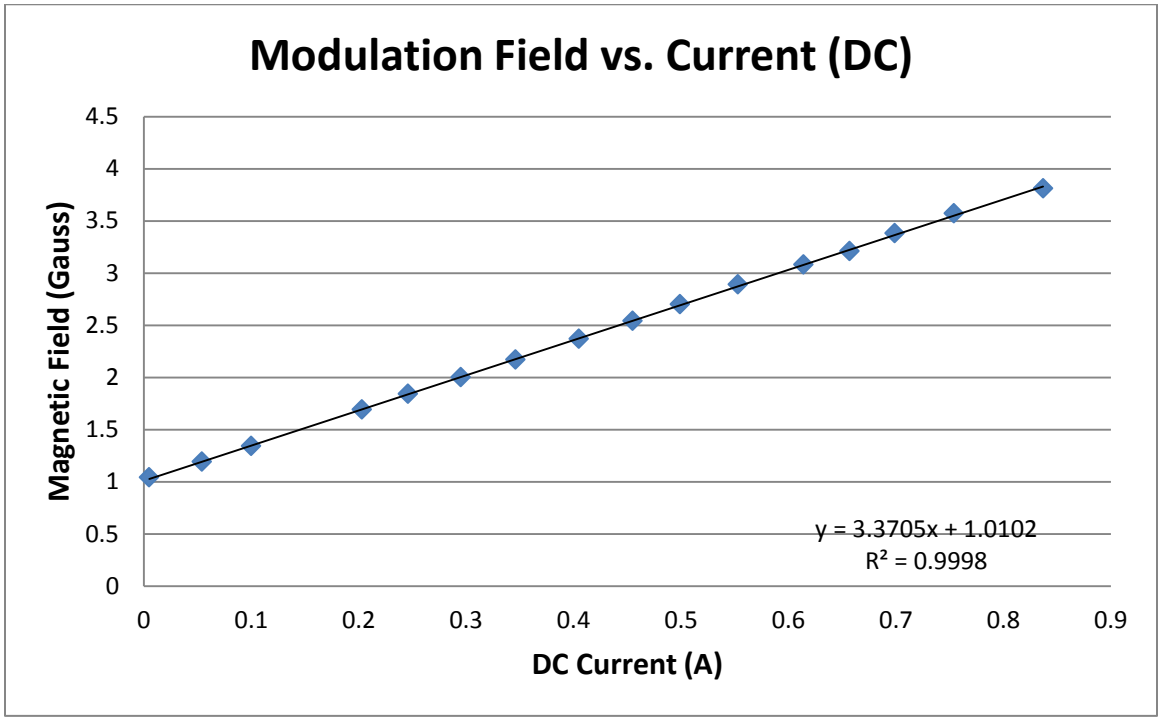

Figure 8: Magnetic Field (Gauss) as a function of DC current (A)

Above is a plot of the modulation coils magnetic field strengths as at different values of DC current. The intercept represents the Earth's magnetic field, indicating a lack of precision in setting the Gauss meter zero. The field scales linearly (with some error in measurement), as we would expect. From this relationship, we can determine what pk-pk current we need to achieve a 4 Gauss modulation, and therefore what pk-pk voltage we must measure from the oscilloscope.

For optimal modulation, the amplitude of the AC signal should be about the same as the width of the SDR signal (in Gauss). Over-modulation provides no additional benefit to the signal-to-noise ratio of the EDMR measurement (and indeed, is likely to damage the equipment being used). Under-modulation results in a decreased signal magnitude. As determined by performing high-field EDMR on SiC MOSFETs, the width of the SDR signal is approximately 4 Gauss.

The function generator output is split to also be used as a reference for the lock-in amplifier, so that it may turn the AC signal back into a DC output.

Magnetic Field Ramp Generation

As discussed above, the magnetic field sweeps from a magnitude of 0 Gauss to about 50 Gauss. Ideally, the waveform is a sawtooth, starting at the minimum value, sweeping linearly to the maximum, and jumping back down to the minimum at the start of the next cycle.

This is obtained by use of a function generator, run through a current-controlled source, and through the large sets of Helmholtz coils. A Lake Shore Gauss meter is used to constantly measure the magnetic field.

Several sources of error in the EDMR measurement are possible within this subsystem. If the signal averager does not begin its trace at the same time as the magnetic field ramp, over the course of signal averaging, it is likely that even a large signal will be averaged out of the final scan because it does not occur at the same time, relative to the beginning of the scan. In actuality, the signal averager does not need to begin the scan at the very start of the magnetic field sweep, or end at the very end of the sweep, just that its position remains fixed in relation to the start of the field sawtooth waveform. The waveform generator provides a synchronizing pulse output in addition to the actual waveform, at the beginning of each period. This is used to trigger the signal

averager to start taking data. The signal averager then is set to end the data set slightly before the actual waveform is complete, so that it does not miss this beginning pulse.

Another possible problem arises if the magnetic field produced by the waveform is not stable over the course of averaging. This issue is indeed the reason for including the current-controlled source. The magnetic field produced by the coils is a direct function of the current running through them, but only indirectly a function of the voltage applied to them. In a perfect world, by Ohm's Law, this would make no difference. In practice, however, running current on the order of 1-2 A through wire will cause significant heating to occur over the course of signal averaging (an hour or more), this in turn, results in a change in the resistance of the wires. Therefore, even if the applied voltage waveform is stable, the signal will appear to "drift" over the course of signal averaging, which in turn will result in the signal averaging process being counterproductive. This potential problem is solved by controlling the current produced by the power supply. The current controlled source serves the function of turning the stable voltage waveform into a corresponding current waveform through the Hemholtz coils, thus correcting for any "drift" before it even happens.

Chapter 3

Results

As of this date, we have yet to obtain a clear, unequivocally true EDMR signal using the low field rig. At various times in the process, we believed we were seeing a signal, but none of these instances proved to be repeatable. We will now discuss several of the problems we encountered over the course of the research, what steps were taken to fix them, highlight an example which we initially believed to show EDMR and the subsequent steps that proved it was not the case. We then speculate on several lingering issues, which may have been the cause for our inability to observe an EDMR signal. Finally, we make an assumption that in the future, an EDMR signal is observed, with better certainty than we currently have now. We discuss the further tests that will be necessary to give a solid grounding to the idea that EDMR on the low field rig is observable, and briefly discuss what could be done next.

Problems encountered

At various points within the project, notable issues were encountered. Individually, any of these would have prevented a signal from being observed. Described below are the problems we encountered and how they were resolved.

The first thing we attempted to fix was the poor physical layout of the setup. Many connecting cables were crossed or unnecessarily long, giving rise to unnecessary sources of noise.

Components from the same subsystem were arranged nearby one another to minimize cable lengths and cable crossing.

The magnetic field controlling signal generator ceased to function. We are uncertain of the exact date of its failure, but it occurred sometime during the fall semester, likely early on in the fall semester. A temporary fix was found in the form of another waveform generator, however this signal generator did not have a sawtooth setting. As a result, we ran it using a triangle wave and recorded both the ramp up and ramp down of magnetic field in the signal averager traces. This was not an ideal fix, because it effectively doubled the time required to average a measurement a given number of times (controlling for speed of magnetic field sweep), but there is no theoretical reason why this would prevent a signal from being seen.

The modulation box quality was low. The box which we were using to start the project was an old, unused, one in the lab and included poor soldering and possible wire shorts. We built a new one from scratch, using only the 10 Ω resistor.

During the week of March 21, 2011, we stopped seeing a characteristic I-V curve from the current preamplifier when changing the device bias. We then believed that the wire bonds must have broken, after re-bonding it, and measuring the device in a parameter analyzer, got a result which made us think that there was a short somewhere on the "T" to which the diode was adhered. Sure enough, we found that the wires in the T were not properly insulated from each other. They were then soldered back on, and fixed in a dried two-part epoxy to ensure the problem would not happen again. We tested the T again, finding no shorts this time, re-bonded the device, and the I-V curve returned.

Also, during the week of March 21, 2011, we noticed a problem when trying to measure the modulation amplitude. We found that the wire connecting the modulation coil to the coaxial connector actually broke. This was most likely due to small bumps and shifts over time, just fatiguing the wire itself. The wire was soldered back on, but this time a small length of extra wire

was added to prevent such a problem from happening again. A multimeter in continuity mode confirmed the new good connection, and the measurements of the modulation returned to normal.

The SiC diode stopped working on March 30, 2011.We first became aware of this problem because the diode was no longer showing proper I-V curve when testing that subsystem. We moved on to test the device itself using a parameter analyzer, and got no response. We replaced the SiC MOSFET with a JFET transistor, which the lab had determined to have a very substantial signal, when run on the larger EDMR rigs.

Recently, we found that the signal averager internal fan has died. As a result, the signal averager now runs the risk of overheating if left on for sustained periods of time (as it did more than once before we realized this was the issue). This is of course a problem, when we wish to average for an hour or more. We took the top off of the machine, hopefully to get better air circulation and keep the machine from overheating. While it hasn't overheated since, we also haven't attempted to run it for any period of time longer than 30 min, by which time, parts of it become too hot to even touch. This is annoying, but it should be possible to obtain a decent signal after only 20 scans or so, and lacking even that, we have not spent time trying to make a component work better, when the system itself has yet to work at all.

Several times, it was found that the RF probe had become de-tuned. This is a simple fix, and just involves finding the new maximum RF frequency.

At various points, we suspected individual pieces of equipment to be malfunctioning Every time, we replaced the part in question with one which was known to work to no new resulting EDMR signal.

Initial promising signs

Below is one test, which initially seemed to be promising. The vertical axis is amplitude (dimensionless), and the horizontal axis is magnetic field scan time. For a linear sawtooth waveform, a time directly corresponds to magnetic field. However, during this test, we were using a triangle waveform to drive the magnetic field (see explanation above). The sweep starts at 0 Gauss on the left, ramps linearly to 34 Gauss, and back down to 0. The signal averager trace ends slightly before the field reaches zero.

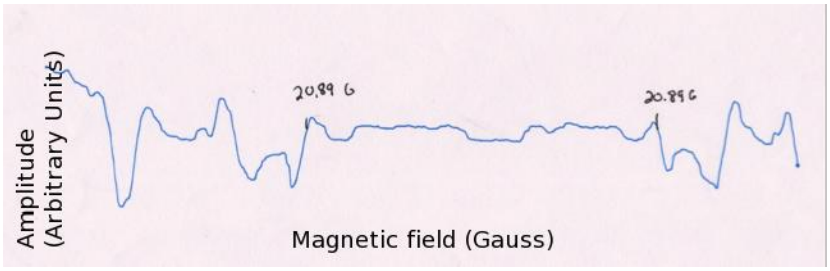

Figure 9: SiC MOSFET under -2.28 V Source/Drain to Substrate, 58.47 MHz RF frequency. Signal Averaged 110 times.

Marked are the two points on the scan where the magnetic field reached 20.89 Gauss, the point where resonance should occur, given a g value of 2. Interesting about this particular test was its apparent symmetric shape. We believed this to be promising in part because, using a triangle waveform for the magnetic field, we would expect the EDMR signal to appear twice, as a mirror image the second time.

After this, we performed the first test to determine if we were really observing EDMR. We ran another test, using the same SiC sample under the same bias with the same modulation for the same number signal averager traces, except with no RF power. If the above test was truly EDMR, without RF power, there will be no resonance and the result observed would be flat.

After the same number of traces, the noise in the signal should average away, showing no features of the magnitude that is seen in the above test.

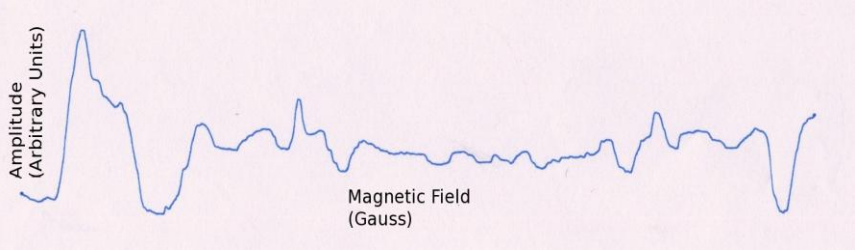

Figure 10: SiC MOSFET, -2.28 V Source/Drain to Substrate, averaged 110 times. No RF power. Vertical scale same as previous.

To our disappointment, turning off the RF power did not significantly diminish all the features present after 110 signal averager traces. With a result such as this, we do not believe that the above test showed an EDMR signal.

Possible Reasons for Failure

While we cannot definitively determine why we are unable to achieve an EDMR signal using the low field rig (if we could, we would have taken steps to fix it), there are several current possible suspects.

When monitoring the modulation waveform through the oscilloscope when all the equipment is running, the resultant figure is not a clean sinusoidal wave. We have determined that the two biggest culprits for this interference are the Kepco current source for the field ramp generation, and the Boonton Signal Generator for the RF power. These both contribute secondary features to the observed modulation waveform. Changing the physical placement of the devices seems ineffective in removing this interference and both pieces of equipment are necessary in the operation of the system, so taking them out or turning them off does nothing to resolve this issue. We are not entirely sure, nor have we been able to definitively test, if this alone would result in

failure to see an EDMR signal. If the modulation coils are not applying a clean sinusoidal waveform, or the lock-in amplifier was not getting a clean reference frequency, an EDMR signal would not be observable. Unfortunately, this particular issue does not seem to have an easy fix.

Future Work

EDMR at Low Fields remains an exciting area of study despite the failure of our work here to obtain an EDMR signal using this rig. In the future use of this rig, if an EDMR signal is believed to have been obtained, several tests are necessary to determine its validity.

First and foremost, the believed signal must be located in a position consistent with the background theory. That is, for the given frequency of RF power, the signal center should reside in a position dictated by $h\nu=g\beta H$. Assuming this is holds, the second step is the same as was conducted here. A second test should be preformed, keeping all parameters constant, with the exception of turning off the RF power. If the result is a noise-free scan showing no significant features after the same number of signal averager traces as the previous test, one would have weak positive confirmation for EDMR. The third test that must be completed, one which we never got to, is to test the same sample under different frequencies of RF power by using different tuned RF probes. For EDMR to be present, the signal must shift in magnetic field to correspond to the new RF frequency. By completing these tests, one would be confident that one is observing EDMR.

Once it is proven that this rig can observe an EDMR signal on a known device, in a manner consistent with conventional EDMR tests on the known device, as well as the background theory, it will be possible to begin testing new devices and make use of the theoretical benefits of low field EDMR.

Chapter 4

Conclusion

The theoretical basis for low field EDMR is sound. Even under non-ideal conditions, assuming that all sub-systems are functioning as they are supposed to, an EDMR signal should be visible. Unfortunately, at the present time, we are unable to demonstrate an EDMR signal, by using the current rig. Upon scrutiny, none of the tests we preformed could be demonstrated to have shown an EDMR signal which was repeatable and consistent with the background theory. We discussed the theoretical benefits of using low magnetic fields for EDMR device characterization, namely equipment cost and high theoretical SNR for wide signal devices. We covered at length, the low field EDMR rig used, highlighting the component systems, as well as tests, which could be preformed on each to ensure that they are operating as we desire. We performed these tests and determined that the components of the rig were operating correctly, and still failed to obtain an EDMR signal when everything was put together. Our tests either failed to show any apparent signal at the magnetic field necessary for resonance, or fell apart after later scrutiny. For the sake of rigor, we explained what further tests would be necessary to prove an apparent signal is, in fact, EDMR and briefly explained how we would proceed after we were satisfied that the rig was operating properly.

Bibliography

[1] D. Kaplan, I. Solomon, and N. F. Mott, J. Phys. (Paris), Lett. 39, L51 (1978).

[2] Cochrane, C.J.. "An electrically detected magnetic resonance study of performance limiting defects in SiC metal oxide semiconductor field effect transistors." *Journal of Applied Physics* 109.1 (2011): 014506. *Jorunal of Applied Physics*. Web. 12 Mar. 2011.

[3] Jander, Albrecht, and Pallavi Dhagat. "Sensitivity Analysis of Magnetic Field Sensors Utilizing Spin-dependent Recombination in Silicon Diodes." Solid State Electronics 54 (2010): 1479-484.

[4] Fukui, Koichi, Toshiyuki Sato, Hidekatsu Yokoyama, Hiroaki Ohya, and Hitoshi Kamada. "Resonance-Field Dependence in Electrically Detected Magnetic Resonance: Effects of Exchange Interaction." Journal of Magnetic Resonance 149 (2001): 13-21. Web.

[5] Tanaka, Hisaaki, Shun-ichiro Watanabe, Kazuhiro Marumoto, and Shin-ichi Kuroda. "Direct Observation of the Charge Carrier Concentration in Organic Field-effect Transistors by Electron Spin Resonance." Journal of Applied Physics 94.10 (2009): 103308. Web.

[6] L. A. Lipkin and J. W. Palmour, IEEE Trans. Electron Devices 46, 525. 1999.

[7] J. A. Cooper, Phys. Status Solidi A 162, 305. 1997.

[8] S. K. Powell, N. Goldsman, J. M. Mc Gairity, J. Bernstein, C. J. Scozzie, and A. J. Lelis, J. Appl. Phys. 92, 4053. 2002.

[9] D. M. Brown, E. Downey, M. Ghezzo, J. Kretchmer, V. Krishnamurthy, W. Hennessy, and G. Michon, Solid-State Electron. 39, 1531.1996.

[10] M. S. Dautrich, P. M. Lenahan, and A. J. Lelis, Appl. Phys. Lett. 89, 223502. 2006.

[11] Cochrane, C. J., P. M. Lenahan, and A. J. Lelis. "Direct Observation of Lifetime Killing Defects in 4H SiC Epitaxial Layers through Spin Dependent Recombination in Bipolar Junction Transistors." Journal of Applied Physics 105.064502 (2009). Jorunal of Applied Physics. Web. 07 Apr. 2011. <http://http://jap.aip.org/>.

[12] J. A. Weil, J. R. Bolton, and J. E. Wertz, Electron Paramagnetic Resonance. Wiley, New York, 1994.

[13] R.Nunlist, Probe tuning techniques http://www.cchem.berkeley.edu/nmr/apps/probetune/probetune.html (1995).

[14]A. S. Grove, Physics and Technology of Semiconductor Devices, (Wiley, New York, 1967).

ACADEMIC VITA OF JOSEPH ACQUAVIVA

Joseph Acquaviva
456 E. Beaver Ave #209
State College, PA 16801
Jpa5045@psu.edu

Education: Bachelor of Engineering Science, Penn State University, Spring 2011
Honors in Engineering Science
Thesis Title: Low Field Electrically Detected Magnetic Resonance
Thesis supervisor: Dr. Patrick M. Lenahan

Related Experience:

Internship with Bridge Semiconductor
Supervisor: Bill Jan
Summer 2008
Worked in the Semiconductor Device Characterization Lab at Penn State
Supervisor: Dr. Patrick M. Lenahan
Summer 2010

Awards:

Dean's List
Schryer Honors College

Presentations/Activities:

ISKF Registered Second Kyu in Shotokan Karate
Won First Place in Collegiate Intermediate Kumite and Second Place in Collegiate Intermediate Kata at 2010 ISKF Nationals
Placed Third Place in Waltz and Tango at the 2010 Yale Ballroom Competition